

## High-resolution Doppler-free two-photon spectroscopic studies of molecules. I. The $\nu_3$ bands of $^{12}\text{CH}_3\text{F}^\dagger$

William K. Bischel\* and Patrick J. Kelly<sup>†</sup>

*Department of Applied Science, University of California, Davis-Livermore, California 94550*

Charles K. Rhodes\*

*Lawrence Livermore Laboratory, University of California, Livermore, California 94550*

(Received 24 November 1975)

We report the first detailed studies of high-resolution Doppler-free two-photon absorption in molecular systems. The  $\nu_3$  vibrational bands in  $^{12}\text{CH}_3\text{F}$  are studied using two fixed-frequency infrared optical fields in combination with molecular Stark tuning. These measurements are used to formulate definite conclusions concerning the free-system properties and collisional interactions in the  $\nu_3$  vibrational manifold. Specifically, the near coincidences of the *P*14 and *P*30 lines of two oppositely directed cw  $\text{CO}_2$  lasers at  $9.6\ \mu\text{m}$  with the  $R(1,1)_{0-\nu_3}$  and the  $R(2,1)_{\nu_3-2\nu_3}$  lines in  $^{12}\text{CH}_3\text{F}$  are used to determine the following properties: (1) precise transition energies for the  $(\nu_3, J, K) = (0, 1, 1) \rightarrow (2, 3, 1)$  two-photon transition, (2) pressure-broadening coefficients, and (3) pressure-shift parameters. Finally, the influence of polarization on the properties of the two-photon signal amplitude is examined.

### I. INTRODUCTION

The general theory of two-photon absorption was initially established by Göppert-Mayer<sup>1</sup> in 1931. The effect, however, was extremely difficult to observe, since the transition probabilities for the available optical intensities were orders of magnitude smaller than single-photon processes. The development of coherent optical sources in 1960 radically changed that situation. Although a number of two-photon experiments were done in the following decade,<sup>2</sup> it wasn't until 1970 that it was suggested that two-photon absorption could be used as a high-resolution tool to perform Doppler-free spectroscopic studies of atomic and molecular systems.<sup>3</sup> It is this application of two-photon absorption (TPA) that is studied here and has since become known as Doppler-free two-photon absorption (DFTPA).

The initial experimental demonstration of DFTPA came in 1974 with simultaneous reports by a number of groups.<sup>4-6</sup> Since that time, DFTPA has found applications to the study of many atomic systems. A good review of much of this recent work can be found in the article by Cagnac.<sup>7</sup> Most of these experimental demonstrations were in the visible-light region in an atomic system using tunable dye lasers. Although the same principles are valid for molecular systems,<sup>8</sup> it is not a trivial exercise to extend the techniques used in the visible to infrared resonances. There are a number of experimental difficulties which make these resonances hard to observe. Included among these

are the relatively smaller infrared transition dipole moments (as compared to typical atomic values), lower detector sensitivities, lack of tunable sources, and insufficient spectroscopic data concerning the excited vibrational manifolds. However, a reasonable class of molecules has been identified which can be used for the initial observation of these DFTPA effects.

Symmetric-top molecules provide a good system for DFTPA since they can have large static dipole moments leading to a large first-order Stark effect. This eliminates the need for tunable lasers. They also generally possess relatively large (compared to typical molecular values) transition dipole moments leading to substantially enhanced TPA cross sections. Finally, the spectroscopy of some well-known symmetric-top molecules (e.g.,  $\text{CH}_3\text{F}$  and  $\text{NH}_3$ ) is sufficiently accurate to be useful for the prediction of two-photon coincidences.

In this work we provide a detailed description of the first observation of DFTPA for molecular systems in the infrared. The initial results of this DFTPA investigation in  $\text{CH}_3\text{F}$  have been reported in Ref. 9(a). We present here a review of this system and additional details not given earlier. The following paper<sup>9(b)</sup> will describe similar observations for the molecular system of  $\text{NH}_3$ .

This paper is organized in the following manner: Section II reviews the perturbative theoretical treatment which leads to TPA coefficients, and its extension to the Doppler-free case. Section III details the experimental apparatus and the results of our measurements in  $\text{CH}_3\text{F}$ , and Sec. IV gives a brief summary of the work.

## II. THEORETICAL DEVELOPMENT OF TWO-PHOTON ABSORPTION

### A. Basic theory

Although the theory of two-photon absorption has been presented by other authors,<sup>2</sup> we include here a perturbative derivation which specifically treats two radiation fields of different frequencies and intensities. Our approach will follow closely that of Göppert-Mayer.<sup>1</sup>

The Hamiltonian for the molecular system can be written

$$\mathcal{H} = \mathcal{H}_0 + \mathcal{H}', \quad (1)$$

where  $\mathcal{H}_0$  is the unperturbed Hamiltonian of the molecule with a complete set of eigenstates  $|n\rangle$  having energies  $E_n$ , and  $\mathcal{H}'$  is the interaction Hamiltonian given by

$$\mathcal{H}' = - (e/mc) \vec{A} \cdot \vec{P} + (e^2/2mc^2) \vec{A} \cdot \vec{A}, \quad (2)$$

in which  $\vec{P}$  is the momentum operation for all the electrons of the system ( $\vec{P} = \sum_i \vec{P}_i$ ) and  $\vec{A}$  is the total vector potential for both radiation fields. Our treatment will assume (1)  $\mathcal{H}'$  to be weak enough so that the behavior of the system can be calculated by perturbation theory, (2) no single-photon transition is possible from either radiation field, and (3) there are no states either  $2\hbar\omega_1$  or  $2\hbar\omega_2$  above the ground state. The absorption of two photons, one coming from each of the two radiation fields, raises the system from its ground state  $|g\rangle$  to a final state  $|f\rangle$  of energy  $E_{fg} = \hbar(\omega_1 + \omega_2)$  above ground state.

From a solution to the Schrödinger equation, the probability amplitude for finding the system in state  $|k\rangle$  at time  $t$  subject to the perturbation  $\mathcal{H}'(t)$  is given by

$$\dot{a}_k^{(1)}(t) = (i\hbar)^{-1} \sum_n \langle k | \mathcal{H}' | n \rangle a_n(t) e^{i\omega_{kn}t}, \quad (3)$$

where  $a_n(t)$  is defined by

$$|\psi\rangle = \sum_n a_n(t) e^{-iE_n t/\hbar} |n\rangle, \quad (4)$$

and  $\omega_{kn} = (E_k - E_n)/\hbar$ . Following the customary procedure for time-dependent perturbation theory<sup>10</sup> we replace  $\mathcal{H}'$  by  $\lambda\mathcal{H}'$  in Eq. (3) and expand  $a_n$  as a power series in  $\lambda$ . Equating powers of the small parameter  $\lambda$  leads to the well-known result

$$\dot{a}_k^{(s)} = (i\hbar)^{-1} \sum_n \langle k | \mathcal{H}' | n \rangle a_n^{(s-1)} e^{i\omega_{kn}t}. \quad (5)$$

We initially assume the system to be in its ground state  $|g\rangle$  [i.e.,  $a_k(0) = \delta_{kg}$ ], leading to the first-order expression

$$\dot{a}_k^{(1)} = (i\hbar)^{-1} \langle k | \mathcal{H}' | g \rangle e^{i\omega_{kg}t}. \quad (6)$$

If the time-dependent part of  $\mathcal{H}'$  is explicitly written

$$\mathcal{H}'(t) = \frac{1}{2} \mathcal{H}'_1 (e^{-i\omega_1 t} + e^{i\omega_1 t}) + \frac{1}{2} \mathcal{H}'_2 (e^{-i\omega_2 t} + e^{i\omega_2 t}), \quad t > 0, \quad (7)$$

$$\mathcal{H}'(t) = 0, \quad t \leq 0,$$

the integration indicated in Eq. (7) can be performed, leading to the first-order result

$$a_k^{(1)} = -\frac{1}{2\hbar} \left( \langle k | \mathcal{H}'_1 | g \rangle \frac{\exp[i(\omega_{kg} - \omega_1)t] - 1}{\omega_{kg} - \omega_1} + \langle k | \mathcal{H}'_2 | g \rangle \frac{\exp[i(\omega_{kg} - \omega_2)t] - 1}{\omega_{kg} - \omega_2} \right), \quad (8)$$

where we have neglected terms with energy denominators of  $\omega_{kg} + \omega_i$ .

Since we are dealing with a two-photon process, we must proceed to second order. Substituting Eq. (8) into Eq. (5) and performing the time integration yields

$$a_f^{(2)}(t) = -\frac{1}{4\hbar} \frac{\exp[i(\omega_{fg} - \omega_1 - \omega_2)t] - 1}{\omega_{fg} - \omega_1 - \omega_2} M^{(2)}, \quad (9)$$

where

$$M^{(2)} = \sum_k \frac{\langle f | \mathcal{H}'_1 | k \rangle \langle k | \mathcal{H}'_2 | g \rangle}{E_{kg} - \hbar\omega_2} + \frac{\langle f | \mathcal{H}'_2 | k \rangle \langle k | \mathcal{H}'_1 | g \rangle}{E_{kg} - \hbar\omega_1} \quad (10)$$

and terms involving  $\omega_{fg} - 2\omega_1$  and  $\omega_{fg} - 2\omega_2$  have been neglected since we originally assumed there were no states having energies  $2\hbar\omega_1$  or  $2\hbar\omega_2$  above the ground state.

The two-photon transition probability is just the square of Eq. (9) and must be averaged over the density of state  $\rho(\omega_{fg})$  clustered about the final state  $|f\rangle$ . For times long compared to the width of  $\rho(\omega_{fg})$ , the integral is easily performed, leading to

$$|a_f^{(2)}(t)|^2 = (\pi/8\hbar^2) |M^{(2)}|^2 \rho(\omega_{fg} = \omega_1 + \omega_2) t. \quad (11)$$

The transition probability rate from the ground state  $|g\rangle$  to the continuum of states near  $|f\rangle$  is thus

$$W_{fg} = \frac{d}{dt} |a_f^{(2)}(t)|^2 = \frac{\pi}{8\hbar^2} |M^{(2)}|^2 \rho(\omega_{fg} = \omega_1 + \omega_2). \quad (12)$$

$M^{(2)}$  in Eq. (12) can be evaluated by transforming the interaction Hamiltonian of Eq. (2) into

$$\mathcal{H}' = -\mu \cdot \vec{E}, \quad (13)$$

where it has been assumed that the  $\vec{A} \cdot \vec{A}$  term does not significantly contribute to the transition probability.<sup>11</sup> Here  $\vec{\mu}$  is the electric dipole moment operator for all the electrons ( $\vec{\mu} = -\sum_i e\vec{r}_i$ ) and  $\vec{E}$  is the total electric field for two plane-wave beams with polarizations denoted by

$$\vec{E} = \frac{1}{2} \{ \hat{\epsilon}_1 E_1 [\exp i(\vec{k}_1 \cdot \vec{r} - \omega_1 t) + \text{c.c.}] + \hat{\epsilon}_2 E_2 [\exp i(\vec{k}_2 \cdot \vec{r} - \omega_2 t) + \text{c.c.}] \}. \quad (14)$$

Here the spectral intensity  $I_i$  is related to the electric field amplitude by

$$|E_i|^2 = (8\pi/c) I_i(\omega_i). \quad (15)$$

Using the dipole approximation ( $e^{i\vec{k} \cdot \vec{r}} \approx 1$ ) and substituting Eqs. (13)–(15) into Eq. (11) yields

$$W_{f_g} = [(2\pi)^3 / \hbar^2 c^2] I_1 I_2 |P_{f_g}|^2 g(\omega_1 + \omega_2), \quad (16)$$

where

$$|P_{f_g}| = \sum_k \frac{\langle f | \hat{\epsilon}_1 \cdot e\vec{r} | k \rangle \langle k | \hat{\epsilon}_2 \cdot e\vec{r} | g \rangle}{E_{kg} - \hbar\omega_1} + \frac{\langle f | \hat{\epsilon}_2 \cdot e\vec{r} | k \rangle \langle k | \hat{\epsilon}_1 \cdot e\vec{r} | g \rangle}{E_{kg} - \hbar\omega_2} \quad (17)$$

and  $\rho(\omega_{kg} = \omega_1 + \omega_2)$  is just the line-shape function  $g(\omega_1 + \omega_2)$ .

As expected, the probability for two-photon absorption is proportional to the intensities of both laser fields. Since experimentally we detect two-photon absorption by monitoring only one of the laser frequencies, it will be convenient to calculate the absorption cross section  $\sigma(\nu_2)$  of a molecule for light at frequency  $\nu_2$  induced by light at  $\nu_1$ . This is given by

$$\frac{dI_2}{dz}(\nu_2) = h\nu_2 W_{f_g} (N_f - N_g) \equiv I_2 \sigma(\nu_2) (N_f - N_g), \quad (18)$$

where  $N_f - N_g$  is the population density difference between the states  $|f\rangle$  and  $|g\rangle$ . Using Eq. (18) we see that the absorption cross section can be calculated from

$$\sigma(\nu_2) = W_{f_g} h\nu_2 / I_2. \quad (19)$$

Substituting Eq. (16) into Eq. (19) and converting the line-shape function  $g(\omega_1 + \omega_2)$  to  $g(\nu_1 + \nu_2)$ , where

$$g(\omega_1 + \omega_2) = (1/2\pi) g(\nu_1 + \nu_2), \quad (20)$$

yields

$$\sigma(\nu_2) = [(2\pi)^3 / \hbar^2 c^2] I_1 \nu_2 |P_{f_g}|^2 g(\nu_1 + \nu_2), \quad (21)$$

giving an absorption coefficient from Eq. (18) of

$$\alpha(\nu_2) = \sigma(\nu_2) (N_f - N_g).$$

A close examination of the composite matrix

element  $P_{f_g}$  [Eq. (17)] provides much information about the processes taking place. The sum is taken over all intermediate states  $|k\rangle$ , although as will be shown later for  $\text{CH}_3\text{F}$  and  $\text{NH}_3$  only one intermediate state provides a significant contribution, because of the resonance denominator. The intermediate state  $|k\rangle$  is required to have dipole matrix elements to both the ground and final states, which implies that both of the latter states must be of the same parity. Since in the absorption process we are unable to distinguish experimentally between absorption of  $\nu_1 + \nu_2$  or its reverse, the amplitudes for both of these processes must be added with the result of both terms in Eq. (17). It is also obvious that the absorption process can be significantly enhanced if one of the frequencies is made close to the transition frequency  $E_{kg}$ . Bjorkholm and Liao<sup>12</sup> showed that in the case of sodium vapor, an increase of over seven orders of magnitude in the two-photon absorption cross section was achieved by just such a technique. Finally, the matrix elements in Eq. (17) depend in an important way on the polarization of the laser fields. These polarization effects can be taken advantage of to eliminate background effects<sup>4</sup> or to observe different two-photon transitions (see Sec. III D).

#### B. Extension of two-photon theory to the Doppler-free case

It has been pointed out<sup>3,13</sup> that the effects of Doppler broadening can be eliminated in two-photon transitions if the two photons have the same energy and are propagating in opposite directions. This effect not only gives narrow linewidths but also enhances the two-photon cross section<sup>8</sup> by a factor  $\Delta\nu_D / \Delta\nu_H$ , where  $\Delta\nu_D$  is the Doppler width defined by [full width at half-maximum (FWHM)]

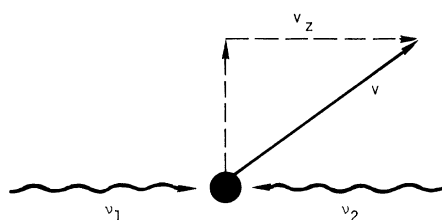
$$\Delta\nu_D = 2(\nu/c)(2 \ln 2 kT/m)^{1/2} \quad (22)$$

and  $\Delta\nu_H$  is the homogeneous width. This factor could be as large as 1000 for molecular systems at low pressures.

To physically understand these processes, we first must transform into the rest frame of the molecule. Here, the molecule sees a radiation field with a frequency defined by

$$\nu' = \nu(1 \pm v_x/c), \quad (23)$$

where  $v_x$  is the molecular velocity along the direction of propagation of the radiation field. This is the normal Doppler shift which limits our spectroscopic resolution. Suppose now that the molecule is subjected to radiation at frequencies  $\nu_1$  and  $\nu_2$  traveling in the  $+z$  and  $-z$  directions, as shown in Fig. 1. The molecule now sees two apparent frequencies, one shifted up and one shifted down. The



A. Doppler shift (rest frame of molecule)

$$\nu' = \nu \left[ 1 \mp \frac{v_z}{c} \right]$$

B. Resonance condition

$$\begin{aligned} \nu_0 &= \nu_1' + \nu_2' \\ \nu_0 &= \nu_1 + \nu_2 + \frac{v_z}{c} (\nu_2 - \nu_1) \end{aligned}$$

C. Residual Doppler linewidth

$$\Delta\nu_D \text{ (FWHM)} = 2 [2 \ln 2]^{1/2} |\nu_2 - \nu_1| \frac{v_z}{c}$$

FIG. 1. Schematic diagram of an atom or molecule having a  $z$  component of velocity  $v_z$  interacting with two oppositely propagating light beams having the frequencies  $\nu_1$  and  $\nu_2$ . Equations A, B, and C give the physical model for the Doppler-free effect described in the text.

resonance condition is satisfied if  $\nu_1'$  and  $\nu_2'$  determined by Eq. (23) add to give the molecular transition frequency  $\nu_0$ . The sum of these two apparent frequencies is

$$\nu_0 = \nu_1' + \nu_2' = \nu_1 + \nu_2 + v_z(\nu_1 - \nu_2)/c. \quad (24)$$

Note that if  $\nu_1 = \nu_2$ , all velocity groups see the same apparent sum frequency and all participate in the absorption process giving the homogeneous value for the linewidth. However, if the two frequencies are not the same, the Doppler width is still reduced by a factor of  $(\nu_1 - \nu_2)/(\nu_1 + \nu_2)$ . This leads to what is known as the residual Doppler width whose value is (FWHM)

$$\Delta\nu_D = 2 |(\nu_1 - \nu_2)/c| (2 \ln 2 kT/m)^{1/2}. \quad (25)$$

This value is on the order of 1 MHz for the cases studied here.

To describe these effects in a more quantitative manner, we follow the treatment first presented in Ref. 14. Note that all linewidth effects are contained in  $g(\nu_1 + \nu_2)$  of Eq. (21). This function can be calculated using techniques similar to those developed by Voigt<sup>15</sup> when he investigated the line shape owing to combined Doppler and homogeneous broadening.

We start by using Eq. (16) to calculate the *veloc-*

*ity*-dependent transition probability

$$W_{fg} = B(\nu_1, \nu_2) I_1 I_2 g(\nu_1 + \nu_2). \quad (26)$$

Here

$$g(\nu_1 + \nu_2) = \frac{1}{\pi} \frac{\frac{1}{2} \Delta\nu_H}{[\nu_1(v) + \nu_2(v) - \nu_0]^2 + (\frac{1}{2} \Delta\nu_H)^2} \quad (27)$$

is the normalized line-shape function for the two-photon transition, where  $\Delta\nu_H = 1/\pi T_2$  is the homogeneous FWHM including collisional effects.

$B(\nu_1, \nu_2)$  is defined by Eq. (16) and  $\nu_1$  and  $\nu_2$  have the velocity dependence described by Eq. (23).

In order to simplify the calculation, we will assume that the homogeneous width ( $\Delta\nu_H$ ) does not depend on the velocity and the energy denominators in  $B(\nu_1, \nu_2)$  are large compared to both the Doppler and the homogeneous widths, making  $B(\nu_1, \nu_2)$  essentially velocity independent.

The number of molecules,  $n(v)$ , contained in width  $\Delta\nu$  at velocity  $v$  is given by the Maxwellian thermal distribution. The number of  $g \rightarrow f$  transitions made by these molecules per unit time and volume is

$$\frac{dn(v)}{dt} = W(\nu_1, \nu_2, v) n(v). \quad (28)$$

The Gaussian thermal distribution of  $n(v)$  for molecules with velocity in the  $z$  direction  $v_z$  (molecules with  $v_x$  and  $v_y$  are always in resonance with the radiation field) is

$$n(v_z) = (n_0/\pi^{1/2} \bar{v}_z) \exp[-(v_z/\bar{v}_z)^2], \quad (29)$$

where  $\bar{v}_z$  is  $\sqrt{2}$  times the average thermal velocity in the  $z$  direction [i.e.,  $\bar{v}_z = (2kT/m)^{1/2}$ ] and  $n_0$  is the total number of molecules in the level of interest and is defined by

$$n_0 = \int_{-\infty}^{\infty} n(v_z) dv_z. \quad (30)$$

The total transition rate per unit volume is obtained by combining Eqs. (26), (28), and (29) and integrating over all velocity groups. Defining  $\delta\nu = \nu_0 - (\nu_1 + \nu_2)$  and  $\Delta\nu = |\nu_1 - \nu_2|$ , we have

$$\int_{-\infty}^{\infty} \frac{dn(v_z)}{dt} dv_z = \frac{dn_0}{dt} = B(\nu_1, \nu_2) I_1 I_2 n_0 g(\nu_1 + \nu_2), \quad (31)$$

where the line-shape function is now defined by

$$g(\nu_1 + \nu_2) = \frac{\frac{1}{2} \Delta\nu_H}{\pi^{3/2} \bar{v}_z} \int_{-\infty}^{\infty} \frac{\exp[-(v_z/\bar{v}_z)^2] dv_z}{(\delta\nu - v_z \Delta\nu/c)^2 + (\frac{1}{2} \Delta\nu_H)^2}. \quad (32)$$

If we define  $t = v_z/\bar{v}_z$ ,  $x = 2\delta\nu(\ln 2)^{1/2}/\Delta\nu_D$ , and  $y = (\Delta\nu_H/\Delta\nu_D)(\ln 2)^{1/2}$ , with  $\Delta\nu_D$  defined by Eq. (25), we can rewrite Eq. (32) as

$$g(\nu_1 + \nu_2) = \frac{2y}{\Delta\nu_H \pi^{3/2}} \int_{-\infty}^{\infty} \frac{ye^{-t^2} dt}{(x-t)^2 + y^2}. \quad (33)$$

This line shape has the form of the well-known Voigt profile. Details concerning this line shape can be found in Ref. 16. The integral in Eq. (33) cannot be evaluated by contour methods on account of the essential singularity arising from the Gaussian. Other methods fail as well, so no known closed-form result is available. However, tabulated values of this function can be found in Ref. 17. There are two limiting cases of Eq. (33) which are of interest. For  $y \ll 1$ , the line-shape function  $g(\nu_1 + \nu_2)$  has the familiar form of a Gaussian. This would fit data at very low pressures. For  $y \gg 1$ , the line is completely pressure broadened and has the usual Lorentzian shape.

### III. EXPERIMENT

#### A. Two-photon transition

Doppler-free two-photon resonances in molecular systems were seen for the first time in the symmetric-top system of  $\text{CH}_3\text{F}$ .<sup>9(a)</sup> This observation was motivated by new laser Stark spectroscopic measurements<sup>18</sup> on the  $\nu_3$  (C-F stretching vibration) bands of  $^{12}\text{CH}_3\text{F}$ . In particular, as shown in Fig. 2, we selected the coincidences of the P14 line with the R(1, 1) transition of the  $0 \rightarrow \nu_3$  fundamental band and the P30 line with the R(2, 1) transi-

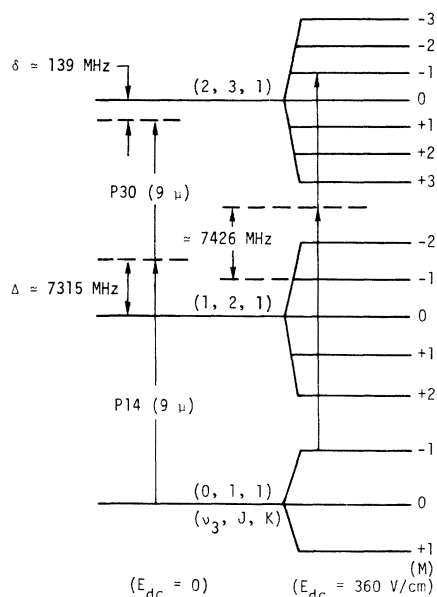


FIG. 2. Two-photon absorption transition in the  $\nu_3$  bands of  $^{12}\text{CH}_3\text{F}$ . The case illustrated is for the two laser photons polarized parallel to the Stark field. This transition can be tuned into resonance using a Stark field of 360 V/cm.

tion of the  $\nu_3 \rightarrow 2\nu_3$  hot band. The frequency difference between the sum of the two laser lines and the selected two-photon transition is  $\sim 139$  MHz. This transition can easily be tuned into resonance by applying a dc Stark field.

The allowed transitions for this parallel band are governed by the selection rules  $\Delta J = \pm 1$ ,  $\Delta K = 0$ , and  $\Delta M = 0, \pm 1$ , depending on the polarization of the laser radiation field and the dc Stark field. Also note that the P14 line is only 7.3 GHz away from the intermediate state. This near resonance condition greatly enhances the TPA cross section.

#### B. Experimental apparatus

A block diagram of the experiment is given in Fig. 3. Two stable  $\text{CO}_2$  lasers (labeled pump and probe oscillators) are locked to a specific frequency within their gain profile on their respective lines (set by experimental conditions) via a local oscillator heterodyning feedback system. The output beams are then propagated through the Stark cell in opposite directions. Care is taken to maximize the overlap region in the Stark cell and yet ensure sufficient exit offset to separate the two beams. Both laser radiation fields are linearly polarized parallel to the dc Stark field and focused to a beam waist of 0.63 mm at the center of the cell. A typical length-averaged pump beam intensity was approximately  $375 \text{ W/cm}^2$ .

The experiment consists of introducing a quantity of gas (approximately 5–150 mTorr of  $\text{CH}_3\text{F}$ ) into the Stark cell and detecting the small amount of absorption of the probe beam by observing the output of a helium-cooled Cu:Ge detector and lock-in amplifier system. The resonance can be swept through by either applying a ramp voltage to the

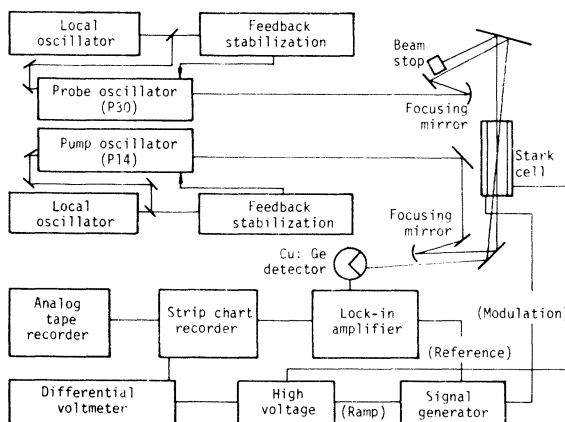


FIG. 3. Schematic diagram of the experimental apparatus.

top plate of the cell via a biased 0–2000-V KEPCO operational amplifier and a signal generator, or by tuning the laser transition by applying a voltage to the piezoelectric crystal on the output mirror of the laser. A small sinusoidal modulating electric field of approximately  $\omega \approx 6$  kHz is applied to the bottom plate of the cell. After passing through the cell, the probe beam is detected synchronously at the modulation frequency  $\omega$  by an ITHACO model 391 lock-in amplifier. The resulting signal is then recorded on magnetic tape for subsequent numerical reduction.

### C. Estimate of TPA cross section in CH<sub>3</sub>F

We can estimate the amount of absorption of the probe beam from Eq. (21). Polarization effects between the radiation fields and the Stark field ( $\Delta M = 0$ , or  $\pm 1$ ) play an important role in the direction-cosine matrix elements of  $P_{fg}$  and have a strong impact on the amplitude of the absorptive process. From tabulated expressions for the matrix elements of symmetric-top molecules<sup>19</sup> it is found that the largest cross section occurs for the parallel-parallel case of  $(J, K, M) = (1, 1, -1) \rightarrow (3, 1, -1)$ , with  $(2, 1, -1)$  constituting the intermediate state. Giving this case the arbitrary value of 100, the relative coupling factor for the other  $\Delta M$  transitions can be calculated by taking the ratio of the squares of the direction-cosine matrix elements. These relative values are given in Table I. Note that in some cases the signal-to-noise ratio can be reduced by a factor of 14 just

TABLE I. Parameters for the CH<sub>3</sub>F two-photon transition of  $J=1, K=1 \rightarrow J=3, K=1$ .

Transition magnetic quantum numbers			Polarization between laser and Stark fields		Relative coupling <sup>a</sup>	Resonant Stark field (V/cm)
$M_g$	$M_i$	$M_f$	$\nu_1$	$\nu_2$		
0	0	1		⊥	50	1770.08
0	1	1	⊥		50	1770.08 <sup>c</sup>
0	1	2	⊥	⊥	33	855.02 <sup>c</sup>
-1	-1	-1			100	360.28 <sup>c</sup>
-1	-1	-2		⊥	63	457.70
-1	-1	0		⊥	20	297.05 <sup>c</sup>
-1	0	0	⊥		20	297.05 <sup>c</sup>
-1 <sup>b</sup>	0	-1	⊥	⊥	28	360.28 <sup>c</sup>
	-2					
-1	0	+1	⊥	⊥	7	360.28
-1	-2	-2	⊥		63	457.70 <sup>c</sup>
-1	-2	-3	⊥	⊥	97	626.61 <sup>c</sup>

<sup>a</sup> These numbers are relative to best-case transition  $(-1, -1, -1)$ , which is given arbitrary value of 100. Coupling is determined by direction-cosine matrix elements.

<sup>b</sup> Includes two intermediate states.

<sup>c</sup> Transitions experimentally observed.

by changing the laser polarization.

Also note that  $P_{fg}$  has a resonant energy denominator. This term can become quite large, as shown in Ref. 12. In this case we are only  $0.25 \text{ cm}^{-1}$  (see Fig. 2) off the intermediate state, leading to a large enhancement of the TPA cross section.

Using Eq. (28) and the experimental parameters tabulated in Table II, we calculate a value of  $\sigma/I$ ,

$$\sigma/I_1 = 3.52 \times 10^{-21} \text{ cm}^2/(\text{W cm}^{-2}).$$

For a pump beam intensity  $I_1 = 375 \text{ W cm}^{-2}$ , an absorption length of  $L = 17.5 \text{ cm}$  and a population difference at 10 mTorr pressure of  $N_f - N_g = 1.22 \times 10^{11} \text{ cm}^{-3}$ , we calculate an absorption of

$$\Delta I_2/I_2 \approx \alpha L = \sigma I_2 (N_f - N_g) = 2.8 \times 10^{-6},$$

or about three parts in  $10^6$ .

It is extremely hard, using our detection techniques, to experimentally measure absolute values for the absorption coefficient. Not only does the amplitude of the absorption signal depend on the amplitude of the modulation voltage applied to the Stark cell, but it also depends on the amount of overlap of the two beams in the cell. If one includes best estimates for these correction factors, we obtain order-of-magnitude agreement with the estimates presented in Table II. We can, however, obtain experimental relative values for the absorption coefficient for the different  $\Delta M$  transition, and these accurately follow ( $\pm 5\%$ ) the ratios predicted in Table I.

### D. Stark tuning of CH<sub>3</sub>F

For the values of electric field strength employed in this experiment, the Stark effect in CH<sub>3</sub>F is predominantly first order with a small but significant second-order correction. In this example of two-photon absorption, we are concerned only with the tuning of the upper ( $f$ ) and lower ( $g$ ) states, since the overall tuning of the transition is then determined by *difference* in these two Stark shifted levels.

The Stark shift of a given level to second order is given by<sup>19</sup>

$$\Delta W(\text{MHz}) = A \mu E + C \mu^2 E^2,$$

where

$$A = aMK/J(J+1),$$

$$C = \frac{a^2}{2B} \left( \frac{(J^2 - K^2)(J^2 - M^2)}{J^3(2J-1)(2J+1)} \right. \quad (34)$$

$$\left. - \frac{[(J+1)^2 - K^2][(J+1)^2 - M^2]}{(J+1)(2J+1)(2J+3)} \right),$$

and  $a = 0.50348$ , such that

$$\vec{\mu} \cdot \vec{E}(\text{MHz}) = 0.50348 \mu(D) E(\text{V/cm}).$$

TABLE II. Two-photon absorption intensity estimates in  $^{12}\text{CH}_3\text{F}$ .

Molecule (transition)	$ μ_{gi} ^2$ (D <sup>2</sup> )	$ μ_{if} ^2$ (D <sup>2</sup> )	$ΔE$ (MHz)	$g(\nu_1 + \nu_2)$ $= 0.94/Δ\nu_D$ ( $\times 10^{-6}$ sec) <sup>a</sup>	$\sigma/I_2$ cm <sup>2</sup> /(W cm <sup>-2</sup> )	$N_g - N_f$ (cm <sup>-3</sup> ) at 10 mTorr	$I_2$ (W/cm <sup>2</sup> )	$L$ (cm)	$\Delta I_2/I_2 = \alpha L$
$\text{CH}_3\text{F}$ (1, 1, -1)									
$\rightarrow(2, 1, -1)$	$6.86 \times 10^{-3}$	0.015	7426	1.0	$3.52 \times 10^{-21}$	$1.22 \times 10^{11}$	375	17.5	$2.8 \times 10^{-6}$
$\rightarrow(3, 1, -1)$									

<sup>a</sup> The transition dipole moment for the  $0 \rightarrow \nu_3$  vibrational mode can be estimated to be 0.19 D from the absolute integrated intensities given by L. A. Gribov and V. N. Smirnov, Usp. Fiz. Nauk 75, 527 (1961) [Sov. Phys. Usp. 4, 919 (1962)]; the residual Doppler width  $\Delta\nu_D$  is calculated from Eq. (25).

If the energy is measured as positive in the vertical direction, then the magnitude of the Stark shift ( $\delta W$ ) necessary to tune the two frequencies ( $\nu_1$  and  $\nu_2$ ) into resonance with the two-photon transition  $\nu_0$  is given by

$$\delta W(\text{MHz}) = (A_g \mu_g - A_f \mu_f)E + (C_g \mu_g^2 - C_f \mu_f^2)E^2, \quad (35)$$

where the subscripts  $g$  and  $f$  refer to the ground and final states, respectively. Since the ground- and final-state dipole moments are well established,<sup>18</sup> Eq. (35) can be reduced to

$$\delta W(\text{MHz}) = D_1 E + D_2 E^2, \quad (36)$$

where

$$D_1 = A_g \mu_g - A_f \mu_f, \quad D_2 = C_g \mu_g^2 - C_f \mu_f^2. \quad (37)$$

These coefficients are evaluated in Table III for the  $\text{CH}_3\text{F}$  two-photon transitions shown in Fig. 2. As can be seen from Eq. (34), the largest tuning results when  $M = J$ . For the case in Fig. 2, the sum of the two  $\text{CO}_2$  photons is below the upper state, leading to  $M = -1$  for the lower state. For

laser fields polarized parallel to the dc Stark field, we have  $\Delta M = 0$  for the selection rule. For this case, we find the tuning in the lower state is six times larger than in the upper state. Note that the second-order corrections indicated in Eq. (34) can be either positive or negative depending on the  $M$  quantum number of the level. The overall tuning calculated from Eq. (36) is approximately 0.385 MHz/(V cm<sup>-1</sup>) for the parallel-parallel case ( $\Delta M = 0$ ).

Other Stark transitions are possible for two-photon transitions with  $\Delta M = \pm 1, \pm 2$ . A list of all of the possible Stark resonances, along with the polarizations between the laser and Stark fields for the transition  $(J, K) = (1, 1) \rightarrow (3, 1)$ , is given in Table I. Also included in Table I are the experimentally determined electric field values necessary to tune the specific two-photon transition into resonance.

To obtain an accurate value of this Stark shift, four quantities must be known: the upper- and lower-state dipole moments, the voltage across the plates, and the plate spacing. The upper- and lower-state dipole moments were determined with

TABLE III. Evaluation of resonant stark shifts in  $\text{CH}_3\text{F}$  for the two-photon transition  $(\nu_3, J, K) = (0, 1, 1) \rightarrow (2, 3, 1)$ .

Transition			$D_1$	$D_2$	$E$	$\delta W$
$M_g$	$M_i$	$M_f$	[MHz/(V cm <sup>-1</sup> )]	[ $10^{-6}$ MHz/(V cm <sup>-1</sup> ) <sup>2</sup> ]	(V/cm) <sup>a</sup>	(MHz)
-1	0	0	0.467 86	-1.609 38	297.05	138.84
-1	-1	-1	0.385 96	-1.517 24	360.28	138.86
-1	-2	-1	0.385 96	-1.517 24	360.28	138.86
-1	-2	-2	0.304 07	-1.240 84	457.70	138.91
-1	-2	-3	0.222 17	-0.780 15	626.61	138.91
0	1	1	0.091 89	-1.945 83	1770.08	138.86
0	1	2	0.163 79	-1.669 42	855.02	138.83
Average						138.87

<sup>a</sup> Taken with 20 mTorr of  $\text{CH}_3\text{F}$ ; plate spacing of  $0.49648 \pm 0.000 10$  cm.

high accuracy in Ref. 18. The voltage is read to one part in  $10^5$  by a Hewlett-Packard differential voltmeter (see Fig. 3). The only unknown quantity is the plate spacing. Our plate spacing was calibrated by varying the locked offset frequencies of both the pump and probe lasers from their respective line centers and observing the Stark voltage required to shift the transition into resonance. Differences in these energy shifts are then calculated using Eqs. (36) and (37). This gave us a plate spacing of  $0.49648 \pm 0.00010$  cm, which is within the experimental error of the measured value.

Once this plate spacing is known, accurate values for the transition frequencies for the various transitions can be calculated from Eq. (36). These determinations are listed in Table III. Since all of the  $M$  levels are degenerate at zero Stark field, these transition frequencies should all be the same. Note that the maximum deviation from the average is only 40 kHz, giving an average transition frequency at 20 mTorr  $\text{CH}_3\text{F}$  pressure of  $\delta W = 138.87$  MHz (see Fig. 2). To obtain the actual transition frequency, this value must be corrected for the pressure shift discussed in Sec. IV F. Making this correction, we obtain a final value for  $\delta W = 138.83$  MHz. Using the values for the frequencies of the two  $\text{CO}_2$  laser photons determined in Ref. 20, we determine a transition frequency for the  $\text{CH}_3\text{F}$  two-photon transition  $(\nu_3, J, K) = (0, 1, 1) - (2, 3, 1)$  of  $2089.634298 \pm 3 \times 10^{-6} \text{ cm}^{-1}$ , giving  $\delta\nu/\nu_0 = 1.6 \times 10^{-9}$ .

#### E. $\text{CH}_3\text{F}$ data analysis

A sample of the data taken using the experimental arrangement of Fig. 3 is given in Fig. 4 for the three different pressures of  $\text{CH}_3\text{F}$  in the Stark cell. The dark line is the actual data taken during the experiment. Note that there is no Doppler background owing to separate beam two-photon absorption, since the frequencies  $2\nu_1$  and  $2\nu_2$  are several hundred Doppler widths off the two-photon resonance. In these figures, the dotted line is the computer fit to the experimental data. Although the theoretical linewidth is a Voigt profile (see Sec. II B), the line-shapes for the case of  $\text{CH}_3\text{F}$  are primarily Lorentzian at pressures greater than 20 mTorr. There is, however, a correction that must be applied to the measured value of the linewidth. This correction results from the large modulation voltage applied to the lower plate of the Stark cell which was necessary for a good signal-to-noise ratio. The "modulation broadening" of a Lorentzian line has been treated theoretically by Wahlquist<sup>21</sup> and, more recently, by Smith.<sup>22</sup> One can obtain a feeling for the value of this correction by noting that their analyses indicate that the reso-

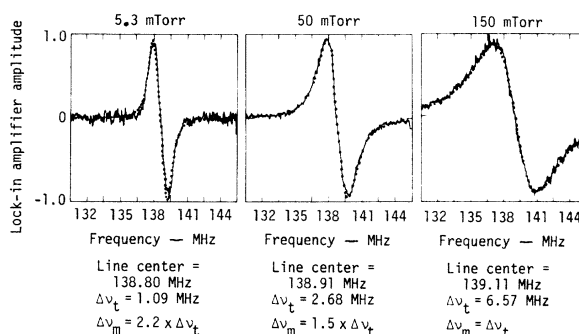


FIG. 4. Examples of pressure-broadening data in  $^{12}\text{CH}_3\text{F}$  for the parallel-parallel two-photon transition  $(J, K, M) \rightarrow (J', K', M')$  of  $(1, 1, -1) \rightarrow (3, 1, -1)$ . All data were taken with a peak-to-peak modulation amplitude of 1.60 MHz. Here  $\Delta\nu_t$  is the true FWHM calculated from our fitting codes, while  $\Delta\nu_m$  is the observed modulation-broadened width. Note there is a "blue" shift in the center frequency of the line as the pressure is increased. This shift is discussed in Sec. III H.

nance is broadened by a factor of 3 when the peak-to-peak modulation amplitude equals twice the true FWHM. This is also the point at which the maximum signal-to-noise ratio occurs. For our experimental conditions, however, we have used a much smaller modulation amplitude. In our analysis, this modulation broadening was taken into account by fitting the observed data to theoretical expressions given in Ref. 22. As indicated in Fig. 4, these fits are quite accurate, indicating that the Lorentzian linewidth approximation is a valid one at pressures above 20 mTorr. The calculation was further checked by taking data at the same pressure but varying the modulation amplitude. All true widths derived from this analysis were within 80 kHz of the average value. Additional broadening mechanisms such as those discussed in Ref. 8 were estimated to contribute less than 100 kHz to the linewidth and were neglected in this analysis.

The widths derived from this analysis are still a convolution of the residual Doppler width and the pressure-broadened width. The homogeneous contribution to these widths was deconvoluted by assuming a residual Doppler width of 0.94 MHz. Plots of the homogeneous contribution versus pressure were then fitted with a straight line to determine the pressure-broadening coefficient. A sample plot of this data for the two-photon transition  $(J, K, M) = (1, 1, -1) \rightarrow (3, 1, -3)$  is given in Fig. 5. Note that the homogeneous contribution extrapolates to near zero, indicating residual line-broadening mechanisms are very small. This stepwise procedure of data analysis was necessary because there are no general theoretical expressions for a line shape which is the modulation-broadened derivative of a Voigt profile. The sim-

plification obtained by assuming the limiting case of a modulation-broadened Lorentzian is justified by the results of the analysis.

This experimental procedure was used to determine two-photon pressure-broadening coefficients for  $\text{CH}_3\text{F}$  for the case of self-broadening for two different  $\Delta M$  transitions. These values are given in Table IV. Note that the pressure-broadening coefficient is smaller for the case of the two laser fields polarized perpendicular to the Stark field. Two foreign-gas perturbers were also used to probe different collisional interactions. These were  $\text{CF}_3\text{I}$  and He. These values are also given in Table IV.

#### F. Line broadening in $\text{CH}_3\text{F}$

Two determinations of  $\text{CH}_3\text{F}$  self-broadening for microwave transitions are available for comparison with the values given in Table IV. The value of the broadening coefficient for the  $J=0 \rightarrow 1$  transition<sup>23</sup> is 40.0 MHz/Torr; for the  $J=2 \rightarrow 3$  transition<sup>24</sup> it is 34.4 MHz/Torr. We observe that our broadening coefficient is very close to these experimental microwave values as we expect, since collisional processes in both the  $\nu_3=0$  and  $\nu_3=2$  vibrational bands should be dominated by rotational relaxation.

One can estimate the linewidth for our two-photon transition using an approximate theory assuming dipole-dipole forces<sup>25</sup> based on Anderson's<sup>26</sup> original pressure-broadening theory of microwave lines. After slightly modifying Eq. (10) of Ref. 25 to account for the fact that we are observing a two-photon transition,<sup>27</sup> we estimate the line-broadening parameter for the  $\text{CH}_3\text{F}$  two-photon transition ( $\nu_3, J, K) = (0, 1, 1) \rightarrow (2, 3, 1)$  to be  $\Delta\nu_p \sim 57$  MHz/Torr. This value is about 36% lar-

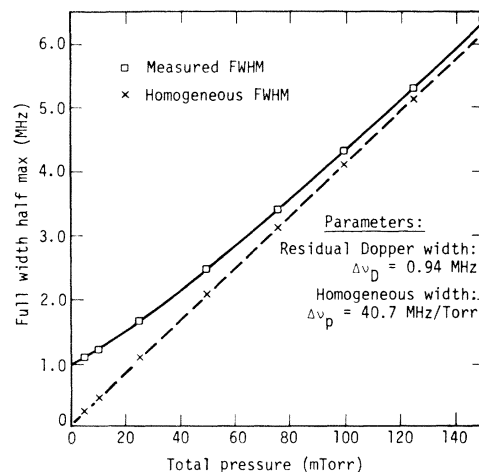


FIG. 5.  $\text{CH}_3\text{F}$  self-broadening data for the two-photon transition  $(J, K, M) \rightarrow (J', K', M')$  of  $(1, 1, -1) \rightarrow (3, 1, -3)$ . The polarizations of the two laser photons were perpendicular to the Stark field. Note that the pressure-broadening coefficient is smaller than the parallel-parallel case given in Table IV.

ger than the experimental value. However, we have overestimated the effect of inelastic collisions because we assumed they were completely resonant. If one calculates the linewidth without the inelastic contribution,  $\Delta\nu_p \sim 32$  MHz/Torr. Hence the experimental number seems reasonable, since it is bracketed by two limiting approximations.

Note that some slight modification in the theory is necessary, since we are actually dealing with nondegenerate  $M$  levels. As can be seen from Table IV, differences at the 3% level are observable in the line-broadening coefficient depending on the initial and final  $M$  values of the radiating molecule.

TABLE IV. Comparison of experimental pressure-broadening parameters in  $^{12}\text{CH}_3\text{F}$  for the two-photon transition  $(\nu_3, J, K, M) = (0, 1, 1, M) \rightarrow (2, 3, 1, M')$ . Conversion formulas:  $\nu_{\text{rel}} = (8kT/\pi\mu)^{1/2}$ ,  $\mu = m_1 m_2 / (m_1 + m_2)$ ; At 300°K; and 1.0 Torr pressure,  $b_e (\text{\AA}) = [\Delta\nu_p (\text{MHz}) / 0.322 \nu_{\text{rel}} (\times 10^{-5})]^{1/2}$ ,  $\sigma (\text{\AA}^2) = \pi b_e^2 (\text{\AA})$ .

Perturber	Radiative transition ( $M \rightarrow M'$ )	Experimental linewidth ( $\Delta\nu_p$ ) (FWHM) (MHz/Torr)	Experimental optical-broadening cross section		Gas kinetic <sup>a</sup> cross section		Reduced mass ( $\mu$ ) (amu)	Relative velocity ( $\nu_{\text{rel}}$ ) ( $\times 10^5$ cm/sec)
			$b_e$ ( $\text{\AA}$ )	$\sigma$ ( $\text{\AA}^2$ )	$b_e$ ( $\text{\AA}$ )	$\sigma$ ( $\text{\AA}^2$ )		
$\text{CH}_3\text{F}$	$-1 \rightarrow -1$	$42.1 \pm 1.0$	16.4	845	4.0 <sup>b</sup>	50.3	17.0	0.485
$\text{CH}_3\text{F}$	$-1 \rightarrow -3$	$40.7 \pm 1.0$	16.1	830	4.0	50.3	17.0	0.485
He	$-1 \rightarrow -1$	$6.3 \pm 0.3$	3.83	46.2	3.29	34.0	3.58	1.33
He	$-1 \rightarrow -3$	$6.0 \pm 0.3$	3.74	44.0	3.29	34.0	3.58	1.33
$\text{CF}_3\text{I}$	$-1 \rightarrow -1$	$46.1 \pm 2.0$	17.5	961	...	...	29.0	0.468

<sup>a</sup> Unless otherwise indicated, the kinetic diameters are those obtained from Joseph O. Hirschfelder, Charles F. Curtis, and R. Byron Bird, *Molecular Theory of Gases and Liquids* (Wiley, New York, 1954). The kinetic diameters for mixtures are obtained from the usual combination rule,  $b = \frac{1}{2}(b_1 + b_2)$ .

<sup>b</sup> G. T. Fogg, P. A. Hanks, and J. D. Lambert, Proc. R. Soc. A 219, 497 (1953).

However, pressure-broadening theories are not well enough developed to predict these small differences in the broadening coefficient.

In addition to the self-broadening data, we have also observed the broadening of  $\text{CH}_3\text{F}$  by foreign-gas perturbers of He and  $\text{CF}_3\text{I}$ . The values obtained are also given in Table IV. Included in this table are conversions of the line-broadening parameter to the effective cross section ( $\sigma$ ) and the effective collision diameter ( $b_e$ ). Note that the optical cross section for self-broadening is larger than that obtained from gas kinetic theory. This can be understood by noting that gas kinetic measurements (i.e., viscosity measurements) require a large transfer of linear momentum during a collision. This happens only when the molecules get close enough for the short-range repulsive forces to become large. This should be compared to the case of the long-range dipole-dipole forces which can transfer angular momentum<sup>28</sup> (rotational-state transitions) without transferring much linear momentum.<sup>29</sup> These arguments immediately lead to the conclusion that the optical-broadening cross sections should be larger than the gas kinetic cross sections. This is not necessarily true for interactions of shorter range. We see from Table IV that for  $\text{CH}_3\text{F}$ -He collisions the value of the two cross sections are close. This can be explained by noting that a short-range interaction with relatively light particles cannot easily transfer angular momentum and cause rotational transitions. Under these conditions, the two cross sections should be approximately the same.

It is interesting to note that both the self-broadening and the helium-broadening coefficients are approximately 3% smaller for the case of the upper state ( $M = -3$ ). Since the lower state ( $M = -1$ ) is the same for both cases, this difference is due to differences in the collisional interaction in the upper state. The estimated error in the absolute value of these broadening parameters is on the order of this difference. However, the relative error is probably much smaller. Although large modifications to existing theories would have to be made to account for this observation, we speculate that one cause might be the fact that three collision channels exist for the upper state of  $(J, K, M) = (3, 1, -1)$  (i.e.,  $\Delta M = 0, \pm 1$ ), whereas only two channels exist for  $(J, K, M) = (3, 1, -3)$  (i.e.,  $\Delta M = 0, +1$ ). This reduction in the number of collisional processes that occur could account for the observed decrease in the linewidth.

One final observation that is unexplained at the present time is that the linewidth parameter for  $\text{CH}_3\text{F}$ - $\text{CF}_3\text{I}$  collisions is larger than the self-broadening, even though  $\text{CF}_3\text{I}$  has a smaller dipole moment<sup>30</sup> (approximately 1 D).

#### G. Pressure-shift observations in $\text{CH}_3\text{F}$

Although a pressure shift of the center frequency of the line is a natural consequence of Anderson's theory,<sup>26</sup> it has not received as much attention as line-broadening studies because these shifts are very difficult to observe in the microwave region. There have, however, been several observations of the pressure shifts in vibrational-rotational lines in the infrared<sup>31</sup> which have stimulated theoretical work in this area.<sup>32</sup>

The main reason for studying these pressure shifts is that they provide information about the intermolecular forces which is different from the information obtained from line-broadening studies. For this we note that the average resonance frequency is determined by the difference in the collisional perturbations in the initial and final states.<sup>33</sup> Also observe that we are probing only those collisional processes which are diagonal in the initial and final states (i.e., no state changes). Those processes which are inelastic and cause state changes will contribute to the broadening of the line but not the shift. Hence line-shift data provide new information on the elastic scattering processes.

As shown in Fig. 3 of Ref. 9(a), we observed a "blue" pressure shift of 2.1 MHz/Torr. This shift is approximately 5% of the broadening parameter. We would expect a shift, since in this case the lower-state dipole moment is fixed in space ( $J=K=1$ ), whereas the upper-state dipole moment is rapidly spinning ( $J=3, K=1$ ). Consequently, the difference in the interaction between the perturbing molecule and these internal motions should lead to a shift, as is experimentally observed. However, this shift cannot be accounted by a simple consideration of dipole-dipole forces. Foley<sup>34</sup> has shown that in this case there should be no shift of the line. This can be understood physically by modeling the collisional field of the perturbing molecule as a time-dependent Stark perturbation. In this case those states with  $+M$  are shifted to lower energies, while the states with  $-M$  are shifted to higher energies, giving no net shift in the center frequency of the line. For our case, additional considerations show that when we are dealing only with a nondegenerate  $M$  level, the average over all field orientations of the perturbing molecule will also lead to a zero shift. This fact was confirmed experimentally in  $\text{CH}_3\text{F}$  by observing *no* pressure shift when using a foreign-gas perturber ( $\text{CF}_3\text{I}$ ) with a reasonable dipole moment ( $\sim 1$  D). This leads us to conclude that the pressure shift must be caused by a resonance contribution to the collisional process which can occur only for the self-broadening case. These resonance contribu-

tions have been used to explain the  $J$  dependence of the line shifts in HCl.<sup>31,32</sup> Recently, Pasmanter and Ben-Reuven<sup>35</sup> have theoretically obtained "blue" pressure shifts of approximately 10% of the linewidth by considering resonant processes involving the transfer of radiation (exchange collisions). Unfortunately, their treatment is not directly applicable to our case, since our initial and final states are not connected by a transition dipole moment. These treatments point out, however, that the process is extremely complicated and our experimental observations are not easily related to any currently existing theory.

#### IV. SUMMARY AND CONCLUSIONS

In conclusion, we have demonstrated that the techniques of Doppler-free two-photon absorption can provide detailed information about the spec-

troscopic and collisional properties of molecular systems. Specifically for CH<sub>3</sub>I we have reported accurate measurements of two-photon transition frequencies [ $(\nu_3, J, K) = (0, 1, 1) \rightarrow (2, 3, 1)$  has been measured to be  $2089.634\,298 \pm 3 \times 10^{-6} \text{ cm}^{-1}$ ], pressure-broadening coefficients for self-broadening and foreign-gas perturbers (see Table IV), and a resonant frequency shift ( $\Delta\nu = 2.1 \pm 0.1 \text{ MHz/Torr}$ ). It is our feeling that these techniques will be extremely useful in studying the excited vibrational manifolds of molecular systems. In fact, a further demonstration of the utility of this approach is given in the following paper<sup>9(b)</sup> for the molecular system of NH<sub>3</sub>.

#### ACKNOWLEDGMENTS

The authors gratefully acknowledge the tireless and expert technical contributions of B. R. Schleicher.

<sup>†</sup>Work performed under the auspices of the U. S. Energy Research and Development Administration.

\*Present address: Molecular Physics Center, Stanford Research Institute, Menlo Park, Calif. 94025.

<sup>‡</sup>Present address: HQ. 15th Engineer Bn., Fort Lewis, Wash. 98433.

<sup>1</sup>M. Göppert-Mayer, *Ann. Phys. (Leipz.)* **9**, 273 (1931).

<sup>2</sup>Reviews of two-photon absorption are presented by A. M. Bonch-Bruевич and V. A. Khodovoi, *Usp. Fiz. Nauk* **85**, 3 (1965) [*Sov. Phys.-Usp.* **8**, 1 (1965)]; A. Gold, in *Quantum Optics, Proceedings of the International School of Physics "Enrico Fermi," Course XLII*, edited by R. J. Glauber (Academic, New York, 1969); J. M. Worlock, in *Laser Handbook*, edited by F. T. Arecchi and E. O. Schulz-DuBois (North-Holland, Amsterdam, 1972); V. I. Bredikhin, M. D. Galanin, and V. N. Genkin, *Usp. Fiz. Nauk* **110**, 3 (1973) [*Sov. Phys.-Usp.* **16**, 299 (1973)].

<sup>3</sup>L. A. Vasileniko, V. P. Chebotaev, and A. V. Shishae, *Zh. Eksp. Teor. Fiz. Pis'ma Red.* **12**, 161 (1970) [*JETP Lett.* **12**, 113 (1970)].

<sup>4</sup>M. D. Levenson and N. Bloembergen, *Phys. Rev. Lett.* **32**, 645 (1974).

<sup>5</sup>F. Biraben, B. Cagnac, and G. Grynberg, *Phys. Rev. Lett.* **32**, 643 (1974).

<sup>6</sup>T. W. Hänsch, K. C. Harvey, G. Meisel, and A. L. Schawlow, *Opt. Commun.* **11**, 50 (1974).

<sup>7</sup>B. Cagnac, in *Laser Spectroscopy* (Springer, Berlin, 1975).

<sup>8</sup>P. L. Kelley, H. Kildal, and H. R. Schlossberg, *Chem. Phys. Lett.* **27**, 62 (1974).

<sup>9</sup>William K. Bischel, Patrick J. Kelly, and Charles K. Rhodes, (a) *Phys. Rev. Lett.* **34**, 300 (1975); (b) follow-up paper, *Phys. Rev. A* **13**, 1829 (1976).

<sup>10</sup>L. I. Schiff, *Quantum Mechanics* (McGraw-Hill, New York, 1972).

<sup>11</sup>R. Guccione and J. van Kranendonk, *Phys. Rev. Lett.* **14**, 583 (1965).

<sup>12</sup>J. E. Bjorkholm and P. F. Liao, *Phys. Rev. Lett.* **33**,

128 (1974).

<sup>13</sup>B. Cagnac, G. Grynberg, and F. Biraben, *J. Phys. (Paris)* **34**, 845 (1973).

<sup>14</sup>J. E. Bjorkholm and P. F. Liao, *IEEE J. Quantum Electron.* **QE-10**, 906 (1974).

<sup>15</sup>W. Voigt, *Munch. Ber.*, p. 603 (1912).

<sup>16</sup>S. S. Penner, *Quantitative Molecular Spectroscopy and Gas Emissivities* (Addison-Wesley, London, 1959); Allan C. G. Mitchell and March W. Zemansky, *Resonance Radiation and Excited Atoms* (Cambridge U.P., Cambridge, 1934).

<sup>17</sup>B. D. Fried and S. D. Conte, *The Plasma Dispersion Function* (Academic, New York, 1961).

<sup>18</sup>S. M. Freund, G. Duxbury, M. Römheld, J. T. Tiedje, and T. Oka, *J. Mol. Spectrosc.* **52**, 38 (1974).

<sup>19</sup>C. H. Townes and A. L. Schawlow, *Microwave Spectroscopy* (McGraw-Hill, New York, 1955).

<sup>20</sup>C. Freed, A. H. M. Ross, and Robert G. O'Donnell, *J. Mol. Spectrosc.* **49**, 438 (1974); F. R. Petersen, D. G. McDonald, F. D. Cupp, and B. L. Danielson, *Phys. Rev. Lett.* **31**, 573 (1973).

<sup>21</sup>Hugo Wahlquist, *J. Chem. Phys.* **35**, 1708 (1961).

<sup>22</sup>R. Lowell Smith, *J. Opt. Soc. Am.* **61**, 1015 (1971).

<sup>23</sup>George Birnbaum, in *Advances in Chemical Physics*, edited by J. O. Hirschfelder (Interscience, New York, 1967), Vol. 12, p. 487.

<sup>24</sup>O. R. Gillian, H. D. Edwards, and W. Gordy, *Phys. Rev.* **75**, 1014 (1949).

<sup>25</sup>George Birnbaum, *J. Chem. Phys.* **46**, 2455 (1967).

<sup>26</sup>P. W. Anderson, *Phys. Rev.* **76**, 647 (1949).

<sup>27</sup>For details of this estimate, see W. K. Bischel, Ph.D. thesis (University of California at Davis, UCRL Report No. 51889, 1975) (unpublished).

<sup>28</sup>F. A. Hopf and C. K. Rhodes, *Phys. Rev. A* **8**, 912 (1973).

<sup>29</sup>See, for example, J. Schmidt, P. R. Berman, and R. G. Brewer, *Phys. Rev. Lett.* **31**, 1103 (1973), where it is estimated that the velocity jump per collision in CH<sub>3</sub>F is 85 cm/sec or 0.2% of the thermal velocity.

- <sup>30</sup>Fred Sterzer, *J. Chem. Phys.* 22, 2094 (1954).
- <sup>31</sup>S. Kimel, M. A. Hirshfeld, and J. H. Jaffe, *J. Chem. Phys.* 31, 81 (1959); J. H. Jaffe, M. A. Hirshfeld, and A. Ben-Reuven, *J. Chem. Phys.* 40, 1705 (1964).
- <sup>32</sup>A. Ben-Reuven, S. Kimel, M. A. Hirshfeld, and J. H. Jaffe, *J. Chem. Phys.* 35, 955 (1961); A. Ben-Reuven, H. Friedman, and J. H. Jaffe, *J. Chem. Phys.* 38, 3021 (1963).
- <sup>33</sup>R. G. Gordon, *J. Chem. Phys.* 44, 3083 (1966).
- <sup>34</sup>H. M. Foley, *Phys. Rev.* 69, 616 (1946).
- <sup>35</sup>R. A. Pasmanter and A. Ben-Reuven, *J. Quant. Spectrosc. Radiat. Transfer* 13, 57 (1973).